

RESEARCH ARTICLE

[View Article Online](#)
[View Journal](#) | [View Issue](#)

 Cite this: *Inorg. Chem. Front.*, 2023,
 10, 3007

A stable nanotubular metal–organic framework as heterogeneous catalyst for efficient chemical fixation of CO₂†

 Xueqin Tian,^{‡a} Xuefu Hu,^{‡b} Wenjing Zhao,^a Pengyan Wu,^{id} *^a Yan Wu,^a Xin Xie,^a
 Fangmin Huang,^{id} *^a Jinwen Cheng^a and Jian Wang^{id} *^a

The incorporation of high-density and easily accessible Lewis acid sites is of great significance to obtain high catalytic activity in the CO₂ cycloaddition reaction of epoxides. Nanotubular metal–organic frameworks (NTMOFs) have attracted widespread attention as heterogeneous catalysts because of their outstanding porosity, intriguing structural diversity and accessible active sites. However, NTMOFs used as heterogeneous catalysts are limited, mainly due to the synthetic difficulties and lack of chemical and physical stability. Herein, we constructed novel NTMOFs with an interior channel diameter of 1.8 nm and an exterior wall diameter of 3.0 nm. They exhibited excellent chemical resistance to both acid and alkaline solutions. The NTMOFs feature durable catalytic performance for CO₂ cycloaddition with epoxides at atmospheric pressure with good recyclability. The turnover frequency (TOF) (306 h⁻¹) value is greater than any previously reported value for metal–organic framework (MOF)-based catalysts for the cycloaddition of CO₂ to epoxides under similar conditions. Experimental results and theoretical calculations reveal that the abundant coordinatively unsaturated open metal sites within the mesoporous nanotubular channels facilitates the sufficient contact of the catalytic active sites with the epoxide substrates, thus enhancing catalytic activity. More importantly, the new materials could be extended to CO₂ fixation by the use of raw power plant flue gas.

 Received 22nd February 2023,
 Accepted 5th April 2023

DOI: 10.1039/d3qi00343d

rsc.li/frontiers-inorganic

Introduction

The chemical conversion of carbon dioxide (CO₂) into valuable organic compounds has attracted great attention for the control of the enormous environmental impact of increasing carbon dioxide concentrations in the atmosphere.¹ This strategy enables the reuse of emitted carbon dioxide to produce a variety of high-value-added chemicals such as organic carbonates,² carboxylic acids,³ carbon oxide,⁴ alkyl amines,⁵ alcohols,⁶ *etc.* It is quite promising for cyclic carbonate production through carbon dioxide cycloaddition with an epoxide in the context of atomic economy and green chemistry because of the widespread application of such products in industry and the

absence of side product generation during this reaction process.⁷ Therefore, catalysts with high activity and heterogeneity are needed for the sustainable application.

Currently, various heterogeneous catalysts have been synthesized and used to promote the cycloaddition reaction of CO₂ with epoxides, including porous carbon,⁸ porous silica,⁹ zeolites,¹⁰ porous organic polymers (POPs),¹¹ *etc.* However, they often are operated under harsh reaction conditions (initial CO₂ pressure >1.0 MPa and/or reaction temperatures >80 °C). There are many reports of this reaction under mild conditions,¹² such as the polar-group-functionalized porous ionic polymer (PIP) POP-PBH,¹³ which could promote the cycloaddition reaction of CO₂ with epichlorohydrin as an efficient bifunctional heterogeneous catalyst with 1.0 mol% catalyst loading at a relatively low temperature (60 °C) and ambient pressure under metal-free conditions during a reaction time of 48 h. Therefore, increasing efforts are being devoted to developing efficient catalysts for the solventless synthesis of cyclic carbonates to take place under milder reaction conditions, including lower initial CO₂ pressure, lower catalyst loading and shorter reaction time.

Crystalline nanotubular metal–organic frameworks (NTMOFs)^{14–19} with the advantages of outstanding porosity, large specific surface area and accessible active sites have

^aJiangsu Key Laboratory of Green Synthetic Chemistry for Functional Materials, School of Chemistry and Materials Science, Jiangsu Normal University, Xuzhou 221116, P. R. China. E-mail: wpyan@jsnu.edu.cn, huangfm@jsnu.edu.cn, wjian@jsnu.edu.cn

^bDepartment of Chemistry, Southern University of Science and Technology, Shenzhen, Guangdong 518055, P. R. China

†Electronic supplementary information (ESI) available: Experimental detail, crystal data, and related spectra. CCDC 2193251. For ESI and crystallographic data in CIF or other electronic format see DOI: <https://doi.org/10.1039/d3qi00343d>

‡These authors contributed equally to this work.

attracted extensive attention, and are widely applied in gas storage,^{20–22} sensing,^{23–25} ice channels,²⁶ magnetic applications,²⁷ small molecular adsorption,^{28–31} encapsulation of guest molecules,³² proton conductivity³³ and catalysis.^{34–36} However, their use has been limited by the synthetic difficulties and lack of chemical and physical stabilities of the NTMOFs. At present, one example of a single-walled metal-organic nanotube based heterogeneous catalyst has been applied in CO₂ cycloaddition with a pressure of 1 MPa at 100 °C for 12 h.³⁵ In order to explore milder-reaction-condition catalytic materials based on NTMOFs, herein, we report the successful design of a nanotube-based metal-organic framework through the solvothermal reaction of propeller-like 4,4',4''-tricarboxyltriphenylamine (H₃tca) and cadmium nitrate, which exhibit high chemical and physical stabilities. The NTMOFs have good carbon dioxide cycloaddition activity within a relatively short reaction time under atmospheric pressure CO₂, which is attributed to the abundant coordination unsaturated cadmium sites located in the pores of the NTMOFs. The reusability of the synthesized NTMOFs and direct CO₂ fixation from raw power plant flue gas were also studied.

Results and discussion

Synthesis and characterization of NTMOF materials

A solvothermal reaction of 4,4',4''-tricarboxyltriphenylamine (H₃tca) with cadmium nitrate in water and *N,N*-dimethyl-

acetamide (DMA) led to a light-yellow block crystalline product, Cd-TCA. Single-crystal X-ray analysis reveals that Cd-TCA crystallizes in the centrosymmetric rhombohedral *R*3̄*c* space group, and it represents a new three-dimensional binodal 3,6-*c* topological network formed by three-fold {4²·6} and six-fold {4⁴·6²·8⁸·10} nodes (in Schläfli notation) (Fig. 1e).³⁷ The asymmetric unit consists of one tca³⁻ ligand, one-and-a-half crystallographically independent Cd(II) cations and one coordinated DMA molecule (Fig. S1, ESI†). The inorganic secondary building unit is a trinuclear Cd cluster (Fig. 1a). The Cd1 atom adopts a perfect hexacoordinated octahedral geometry (Cd–O: 2.242–2.261 Å), is located at the centre of symmetry, and coordinates with four O atoms from four different tca³⁻ ligands through four monodentate μ₂-η¹:η¹ modes and two bridging μ₂-η²:η¹ modes (Fig. S2a, ESI†).

The two equivalent terminal Cd2 atoms in the SBU are five-coordinated with a triangular pyramidal environment; four of them come from the carboxylate oxygen atoms of tca³⁻ ligands, and the fifth is the oxygen atom of a coordinating DMA solvent molecule. The Cd...Cd separation is 3.64(3) Å. The interphenyl dihedral angles for the tca³⁻ ligand are 60.7(1)°, 68.3(7)° and 74.9(6)° with a μ₆-η¹:η¹:η¹:η¹:η¹:η² coordination mode (Fig. S2b, ESI†). The extended coordination of six such trinuclear cadmium SBUs by the carboxyl groups of the tca³⁻ ligands results in the formation of “crown ether”-like hexagonal metallo-macrocycles, which are further connected infinitely with adjacent channels along the *ab* plane sharing the corrugated walls, forming NTMOFs having an outer diameter of 30 Å and an effective pore size of approximately 18 Å

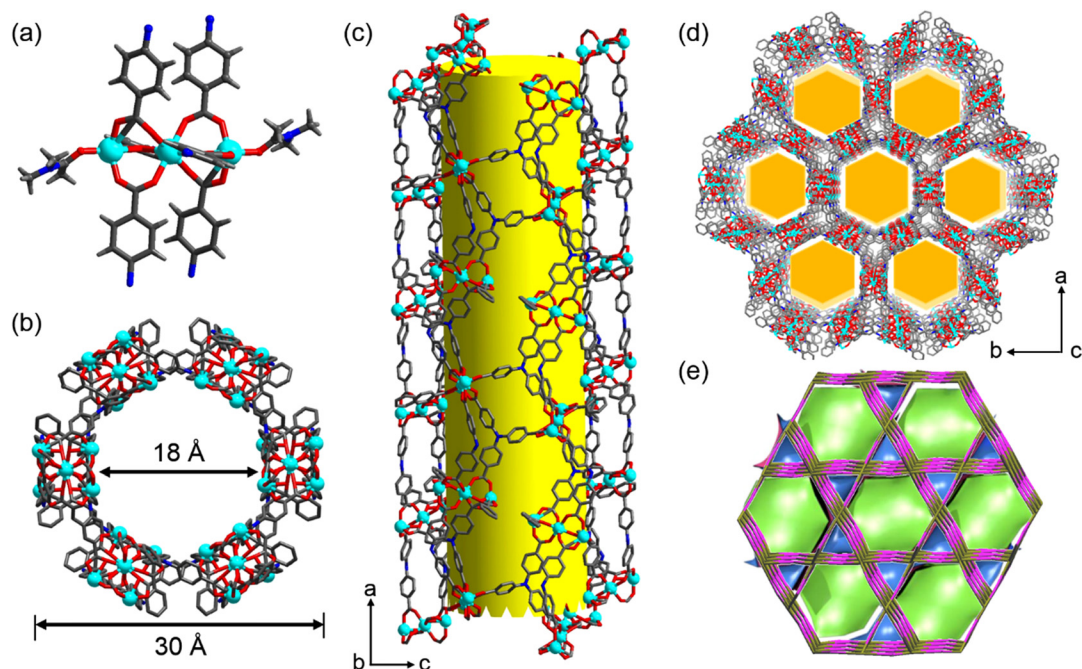


Fig. 1 (a) Cd coordination environment in Cd-TCA. (b) Each nanochannel is composed of trinuclear cadmium SBUs that are linked through tca³⁻ ligands (H atoms are omitted for clarity). (c) Nanotubular structure of Cd-TCA showing the tube interior (yellow column) along the *b* direction. (d) Packing diagram of Cd-TCA with 1D opening channels along the *c* direction. (e) The 3,6-*c* topology for the NTMOF structure in Cd-TCA (the light-green and violet nodes in the network represent Cd(II) ions and the center of the tca³⁻ ligands, respectively).

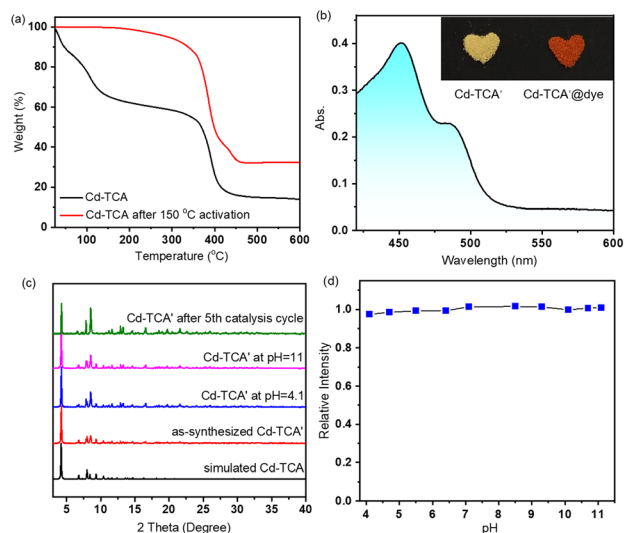


Fig. 2 (a) The TG curve of Cd-TCA from room temperature to 600 °C. (b) UV-vis monitoring of 2',7'-dichlorofluorescein dye released from Cd-TCA'. Inset: optical photographs showing the solids of Cd-TCA' (left) and Cd-TCA' after 2',7'-dichlorofluorescein soaking treatment (right). (c) Powder XRD patterns: simulation from Cd-TCA single-crystal data, as-synthesized Cd-TCA', Cd-TCA' immersed in solutions with different pH values and Cd-TCA' after catalysis. (d) Fluorescence intensity of Cd-TCA' at different pH values in water.

(Fig. 1b–d and Fig. S3, ESI†). The topological analysis of Cd-TCA using ToposPro showed that the Cd_3O SBUs can be regarded as six connected nodes and the tca^{3-} ligands can be regarded as three connected nodes. The point symbol for the net of Cd-TCA is $\{4^2 \cdot 6\}^2 \{4^4 \cdot 6^2 \cdot 8^8 \cdot 10\}$; it possesses a novel topology 3,6-c net with stoichiometry (3-c)2(6-c) (2-nodal net; Fig. 1e). The solvent cavity calculated using the program Platon is 57.4% of the total crystal volume. TGA of Cd-TCA shows that a weight loss of 40.5% was observed between 30 and 200 °C, corresponding to the loss of DMA molecules (expected: 39.6%) (Fig. 2a). These results are perfectly consistent with the elemental analysis data.

The activated compound Cd-TCA' was generated through the desolvation process by heating as-synthesized Cd-TCA at 150 °C under vacuum for 12 h, and the resulting PXRD pattern indicated that the host framework remained stable after removing the guest molecules (Fig. 2c). TGA and FT-IR also clearly indicated that the coordinated DMA molecules were completely excluded (Fig. 2a and S4 in ESI†). These coordinatively unsaturated open metal sites are conducive to interaction with guest molecules that enter the framework pores. The porosity of Cd-TCA' was tested using activated samples *via* dye-sorption measurements. Cd-TCA' samples were soaked in a methanol solution of 2',7'-dichlorofluorescein, and the filtered solids demonstrated obvious adsorption capacity for these dyes *via* UV-vis absorption spectrum monitoring. This experiment gave a quantum uptake equivalent to 6.6% of the Cd-TCA' weight (Fig. 2b), and the Cd-TCA' samples showed an obvious color change from yellow to orange after 2',7'-dichlorofluorescein soaking treatment (Fig. 2b, insert), all of which

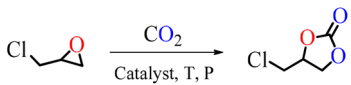
indicated that the channels of the Cd-TCA' are accessible to large reagents typically used for catalysis, as the dye molecules have very large estimated cross-sections. The nanotubular channel structure in Cd-TCA' is conducive to the full exposure of the abundant coordinatively unsaturated open metal sites in the channels to facilitate sufficient contact of the catalytic active sites with the epoxide substrates to enhance catalytic activity, suggesting that Cd-TCA' should function as an active heterogeneous catalyst for the cycloaddition of carbon dioxide.

In order to explore the chemical resistance of Cd-TCA', Cd-TCA' samples were placed in a pH = 4.1 or pH = 11 aqueous solution for one day. The structures of the samples were evaluated using powder XRD (Fig. 2c). It is noted that Cd-TCA' was stable under these two tested conditions, and thus its structural and chemical integrity at different pH values can be confirmed. Additionally, investigation of the pH-dependent fluorescence response of Cd-TCA' showed that there was almost no change in its emission intensity in the pH range of 4.1–11.1 (Fig. 2d). Encouraged by considerably high thermal stability and chemical stability, the catalytic activities of the NTMOFs were further studied.

Catalytic performance in the cycloaddition of CO_2 to epoxides

Our catalytic experiments focused on CO_2 cycloaddition to epoxides, and the optimized catalyst dosage was 1.8 μmol and reaction temperature was 60 °C under 1 atm CO_2 (Fig. S5, ESI†). The initial catalytic activity was assessed with epichlorohydrin (3.3 mmol) as the substrate and CO_2 (balloon pressure, 1 atm), using 1.8 μmol (5.5 mmol%) Cd-TCA', in the presence of tetrabutylammonium bromide (TBABr, 0.3 mmol) as the co-catalyst at a temperature of 60 °C in a solvent-free environment. As can be seen from Table 2, an almost complete conversion can be achieved within 6 h over Cd-TCA' (entry 1 in Table 2). The yields of the cyclic carbonates from a small aliquot of the supernatant reaction mixture were calculated using ^1H NMR. The turnover number (TON) per mole of Cd-TCA' for epichlorohydrin was about 1833, while the turnover frequency (TOF) per mole of Cd-TCA' per hour for epichlorohydrin was approximately 306. To the best of our knowledge, this TOF value is greater than any previously reported value for MOF-based catalysts for the cycloaddition of CO_2 to epoxides under similar conditions (see Table S3 in ESI for comparison†).

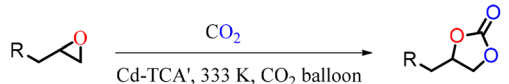
Control experiments were further carried out to investigate the factors influencing this reaction in detail. No 4-(chloromethyl)-1,3-dioxolan-2-one product was generated in the absence of catalysts (Table 1, entry 1). Cd-TCA' or cadmium nitrate resulted in only 2% and 6% catalytic yield without a co-catalyst under the desired conditions (Table 1, entries 2 and 3). When TBABr alone was used as the catalyst, the activity was also negligible (Table 1, entry 4). Furthermore, the subcomponents of Cd-TCA' were then investigated independently. In the presence of 4,4',4''-tricarboxyltriphenylamine (H_3tca) or cadmium nitrate instead of Cd-TCA', the conversion of epichlorohydrin was sharply reduced to 7% and 45%, respectively, under the same conditions (Table 1, entries 5 and 6). Thus, these results demonstrated that our Cd-TCA' was essential for CO_2 cycloaddition reaction with epoxides.

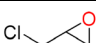
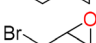
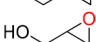
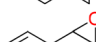
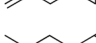
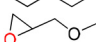
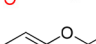
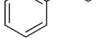
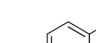
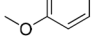
Table 1 Control experiments of coupling of epichlorohydrin with CO₂^a


Entry	Catalyst	Co-catalyst	Yield ^b (%)
1	None	None	n.d.
2	Cd-TCA'	None	2
3	Cd(NO ₃) ₂	None	6
4	None	TBABr	n.d.
5	H ₃ tca	TBABr	7
6	Cd(NO ₃) ₂	TBABr	45

^a Reaction conditions: epichlorohydrin (3.3 mmol), catalyst (1.8 μmol based on Cd_{1.5}, 1.8 μmol based on H₃tca, and 2.7 μmol based on Cd(NO₃)₂), and TBABr (0.3 mmol) with 1 atm CO₂ at 333 K for 6 h. ^b The yield of products was determined using ¹H NMR.

To assess the applicability of Cd-TCA' catalyst, CO₂ cycloaddition to different epoxides (Table S4, ESI[†]) was carried out under similar conditions. As shown in Table 2, the reaction yields catalyzed by Cd-TCA' from related aliphatic epoxides were 98% for epibromohydrin, 100% for glycidol, 93% for allyl glycidyl ether, 92% for butyl glycidyl ether and 97% for glycol diglycidyl ether with corresponding TOF values of 299, 306, 284, 281 and 296 per h per Cd_{1.5} cluster, respectively (Table 2, entries 2–6). When the benzene-containing molecules 2-(phe-

Table 2 Cd-TCA' catalyzed coupling of epoxides with CO₂^a


Entry	Epoxides	Yield ^b (%)	TON ^c	TOF ^d
1		100	1833	306
2		98	1796	299
3		100	1833	306
4		93	1705	284
5		92	1687	281
6		97	1778	296
7		97	1778	296
8		78	1430	238
9		86	1577	263
10		72	1320	220

^a Reaction conditions: Cd-TCA' (1.8 μmol, based on Cd_{1.5}), epoxide (3.3 mmol), and TBABr (0.3 mmol) with 1 atm CO₂ at 333 K and 6.0 h. ^b The yield of products was determined by ¹H NMR. ^c Moles of product per mole of Cd-TCA'. ^d Moles of product per mole of Cd-TCA' per hour.

noxy)methyl]oxirane, 2-((4-methoxyphenoxy)methyl)-oxirane, 2-[[4-nitrophenoxy)methyl]oxirane and resorcinol diglycidyl ether were used as substrates, the epoxy carbonates were produced with yields reaching 97%, 78%, 86% and 72% and corresponding TOF values of 296, 238, 263 and 220 per h per Cd_{1.5} cluster, respectively (Table 2, entries 7–10). Thus, all the epoxides exhibit high yields (>70%). These results demonstrated that Cd-TCA' displays excellent performance in this catalytic transformation of CO₂ to cyclic carbonates due to its large mesoporous diameter, which is beneficial for the substrates to sufficiently come into contact with the catalytic active sites. The recycling behavior of Cd-TCA' in the CO₂ fixation reaction of epichlorohydrin was studied in five consecutive runs. After each catalysis, Cd-TCA' was collected by centrifugation and washed with diethyl ether, dried under vacuum, and reused for the next catalytic run. There was almost no observable change in the catalytic activity of the Cd-TCA' catalyst; the yield of the product 4-(chloromethyl)-1,3-dioxolane-2-one remained at about 98% for five consecutive runs (Fig. 5a). Furthermore, the PXRD result exhibited barely any difference before and after the catalytic reaction (Fig. 2c), explicitly confirming the structural stability of the Cd-TCA' during catalysis, which was also further supported by the SEM images (Fig. S6, ESI[†]). In addition, the leaching of Cd in this reaction system as determined using inductively coupled plasma (ICP) analysis was also very low (<1%), which further verified the heterogeneity of Cd-TCA'. All of the above results suggest the favorable stability of Cd-TCA', which is very important for practical applications. Therefore, since Cd-TCA' has high stability and good recyclability, we carried out a gram-scale experiment for the fixation reaction of epichlorohydrin and CO₂ catalyzed by Cd-TCA'. The reaction was performed by adding 10 mmol of epichlorohydrin and extending the reaction time to 18 h; the other reaction conditions were not changed. It is worth noting that a yield of up to 97.1% can be achieved, giving a total of 1.33 g of product.

Mechanism study

Previous experimental and theoretical studies have demonstrated that the ring-opening of the epoxide was the rate-determining step for the cycloaddition reaction.^{38,39} Thus, the activation of epoxide by Cd-TCA' was first studied. The FT-IR spectra of Cd-TCA' after immersion in a methanol solution of epichlorohydrin displayed the C–H stretching vibration at the range from 2963 to 2860 cm⁻¹, with an apparent red-shift from the range of 3066 to 2921 cm⁻¹ (free epichlorohydrin), indicating that the epoxide can be adsorbed and activated by Cd-TCA' (Fig. S7, ESI[†]).

Additionally, XPS spectra further illustrated the coordination environment of Cd in Cd-TCA' before and after immersion in an epichlorohydrin solution. The Cd 2d spectra suggested a positive shift for Cd-TCA' after immersion in epichlorohydrin (two peaks at 405.79 eV and 412.66 eV), compared with that for Cd-TCA' (405.58 eV and 412.38 eV) (Fig. 3a, insert). This result should be attributed to the decreased electron density around the Cd atoms, which most probably

derived from the weak bonding interaction between the Cd^{2+} center and epichlorohydrin.⁴⁰ A new peak of Cl 2p could be found in the XPS full spectrum of Cd-TCA' (Fig. 3a), which further confirmed that epichlorohydrin was adsorbed into the Cd-TCA'. Extensive molecular-force-field-based calculations were implemented for Cd-TCA' in order to monitor its affinity toward epichlorohydrin. Bonding interactions were observed between Cd centers and the O atom of epichlorohydrin, with the shortest interatomic separation being 2.53(7) Å (Fig. 3b). Additionally, SEM images revealed retention of the morphology without the formation of surface-deposited solids throughout the epichlorohydrin immersion process (Fig. 3c and d). Moreover, the EDX elemental mapping revealed that Cd and Cl are uniformly distributed in epichlorohydrin-treated Cd-TCA' (Fig. 3e). All the results supported the conclusion that Cd-TCA' could adsorb and activate epichlorohydrin.

Based on the experimental results and previous reports,^{7,35,41,42} a Cd-TCA'-catalyzed CO_2 cycloaddition process is proposed (Fig. 4). First, the epoxide binds to the Lewis acid sites in Cd-TCA' through the O atom of the epoxide, which leads to the activation of the epoxy ring. The carbon atom with less steric hindrance is attacked by Br^- that is generated from TBABr to open the epoxy ring. The oxygen anion on the opened epoxy ring then combines with carbon dioxide to form an alkyl carbonate anion. Finally, cyclization occurs *via* intramolecular nucleophilic substitution to generate the cyclic car-

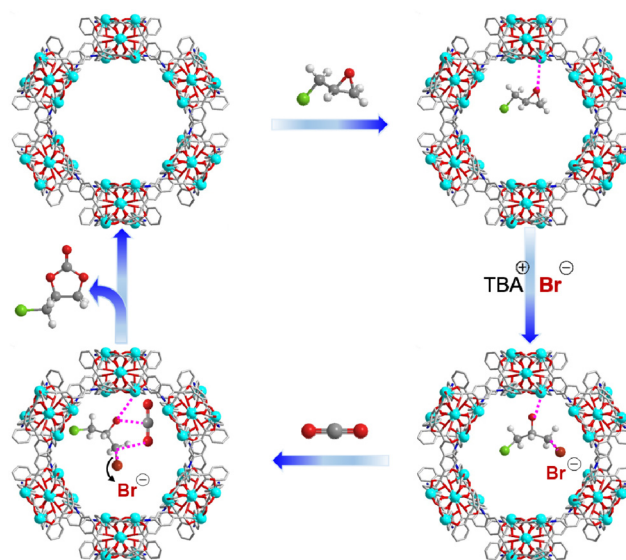


Fig. 4 Proposed mechanism of Cd-TCA'-catalyzed CO_2 cycloaddition with epoxides.

bonate and regenerate the catalytic species to complete the catalytic cycle.

CO_2 cycloaddition of epoxides using mixed gases

Coal-fired power stations are the main source of CO_2 accumulation in the Earth's atmosphere. The exhaust gas emitted by coal-fired power stations is a mixture of about 80% N_2 , 14% CO_2 and 6% O_2 .⁴³ We decided to further explore the application of Cd-TCA' in CO_2 fixation in simulated samples by simulating the above mixed gas. Under the same experimental conditions, except that mixed gases (1.0 MPa, ensuring that the CO_2 pressure is about 1 atm) were used instead of high-purity CO_2 gas, the yield of the product 4-(chloromethyl)-1,3-dioxolan-2-one was 91.4% (Fig. 5b). This efficiency is almost consistent with that using pure CO_2 gas, indicating that the activity of the catalyst in CO_2 chemical fixation was not decreased due to the use of the mixed gases without further separation and purification. In addition, the typical components of coal-fired flue gas are 76.0–77.0% N_2 , 12.5%–12.8% CO_2 , 4.4% O_2 , 6.2% H_2O , 420 ppm NO_x , 50 ppm CO and 420 ppm SO_2 .^{44,45} In terms of studying the catalytic conversion application of carbon dioxide in actual samples, the influence of N_2 and trace gases (SO_2 , NO_x , CO) can be ignored, and O_2 and H_2O may have the greatest impact on the reaction. In order to promote the practical application of this material in industry, the catalytic conversion of CO_2 using high-purity CO_2 and mixed gases in the presence of moisture (100 μL) was also explored. The yield of the product 4-(chloromethyl)-1,3-dioxolan-2-one was 97.3% and 83.6% using high-purity CO_2 and mixed gas, respectively, demonstrating that the catalyst activity was not affected by moisture, and Cd-TCA' has clear feasibility for practical application in the chemical industry.

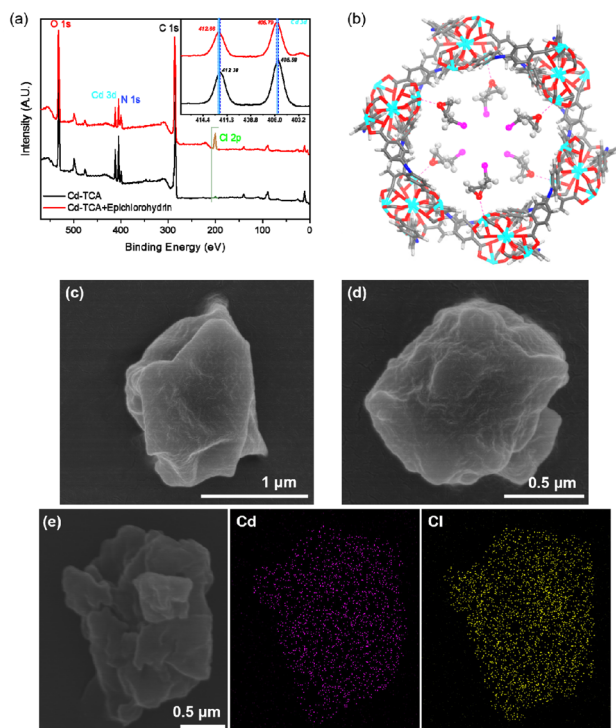


Fig. 3 (a) XPS spectra for Cd-TCA' and Cd-TCA' after treated with epichlorohydrin. Insert shows the Cd 3d region of Cd-TCA' and Cd-TCA' after immersion in an epichlorohydrin solution. (b) The calculated interaction between Cd-TCA' and epichlorohydrin. (c and d) SEM images of Cd-TCA' and epichlorohydrin-treated Cd-TCA'. (e) SEM/EDX images of epichlorohydrin-treated Cd-TCA'.

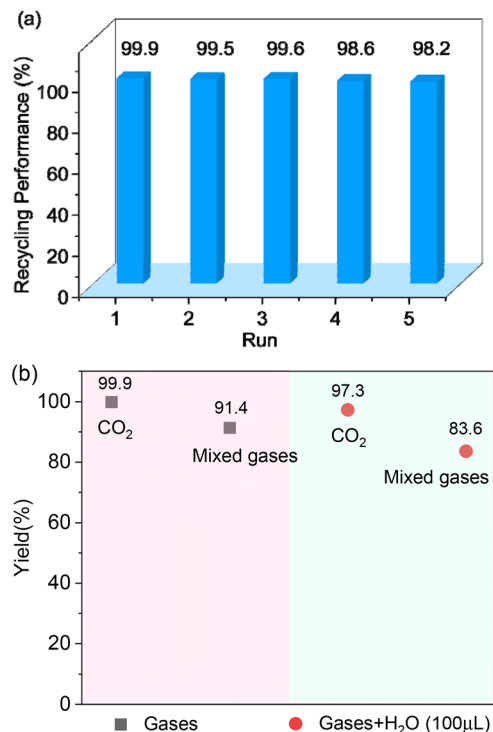


Fig. 5 (a) Recycling experiment of Cd-TCA' for CO₂ cycloaddition with epichlorohydrin. (b) CO₂ cycloaddition of epoxides using mixed gases and mixed wet gases, respectively.

Conclusions

In conclusion, we have successfully prepared a new nanotubular metal-organic framework material with the propeller-like triphenylamine moiety as the backbone, and it possesses a new 3,6-conn topology and can act as a heterogeneous catalyst for CO₂ cycloaddition with various epoxides. It features strong stability and superior catalytic performance with the highest activity of a turnover frequency reaching 1500 per mole of catalyst per hour after five repeated reactions using a CO₂ balloon. The high-density and easily accessible Lewis acid sites within the mesoporous nanotubular channels facilitate sufficient contact of the catalytic active sites with the substrates, thus enhancing catalytic activity. It is worth noting that this material can also be applied to simulate the fixation of actual CO₂ gas in raw power station flue gas. This work provides an efficient approach to use the nanotubes for the CO₂ cycloaddition reaction with cyclic carbonates under mild conditions.

Experimental

Synthesis of Cd-TCA

A mixture of H₂O/*N,N*-dimethylacetamide (10 mL) containing 4,4',4''-tricarboxyltriphenylamine (H₃tca) (23.0 mg) and Cd (NO₃)₂·4H₂O (88.0 mg) was placed in an oven and heated at 110 °C for 2 days; when cooled, light-yellow bulk crystals were produced and collected. Yield: 76%. Anal calc. for [Cd_{1.5}(tca)

(DMA)]₃DMA (C₃₇H₄₈N₅O₁₀Cd_{1.5}): C 49.85, H 5.43, N 7.86%; found: C 49.72, H 5.38, N 7.77%.

Typical procedure for the CO₂ cycloaddition reaction with epoxides

In a 10 mL Schlenk tube, the catalytic reaction was performed with a steady reaction tube pressure controlled by a rubber bladder containing CO₂ (0.1 MPa). The catalyst Cd-TCA' (1.8 µmol, 5.5 mmol%, based on Cd_{1.5}), epoxide (3.3 mmol), and the cocatalyst tetra-*n-tert*-butylammonium bromide (TBAB, 0.3 mmol) were added, and the reaction mixture was stirred at 333 K for 6.0 h. When the reaction was completed, the supernatant solution obtained after the catalysts were centrifuged was used for ¹H NMR analysis, and the reaction yields were calculated.

Conflicts of interest

There are no conflicts to declare.

Acknowledgements

We gratefully acknowledge financial support from the Major Basic Research Project of the Natural Science Foundation of the Jiangsu Higher Education Institutions (No. 21KJA150001), the Natural Science Foundation of Jiangsu Province for Outstanding Youth (No. BK20180105), TAPP of Jiangsu Higher Education Institutions, and the Postgraduate Research & Practice Innovation Program of Jiangsu Normal University.

References

- C. A. Trickett, A. Helal, B. A. Al-Maythaly, Z. H. Yamani, K. E. Cordova and O. M. Yaghi, The chemistry of metal-organic frameworks for CO₂ capture, regeneration and conversion, *Nat. Rev. Mater.*, 2017, **2**, 17045.
- J. Liang, Y.-B. Huang and R. Cao, Metal-organic frameworks and porous organic polymers for sustainable fixation of carbon dioxide into cyclic carbonates, *Coord. Chem. Rev.*, 2019, **378**, 32–65.
- Y. Fu, D. Sun, Y. Chen, R. Huang, Z. Ding, X. Fu and Z. Li, An Amine-Functionalized Titanium Metal-Organic Framework Photocatalyst with Visible-Light-Induced Activity for CO₂ Reduction, *Angew. Chem., Int. Ed.*, 2012, **51**, 3364–3367.
- W.-G. Cui, G.-Y. Zhang, T.-L. Hu and X.-H. Bu, Metal-organic framework-based heterogeneous catalysts for the conversion of C1 chemistry: CO, CO₂ and CH₄, *Coord. Chem. Rev.*, 2019, **387**, 79–120.
- X.-R. Tian, X.-L. Jiang, S.-L. Hou, Z.-H. Jiao, J. Han and B. Zhao, Selectively Regulating Lewis Acid-Base Sites in Metal-Organic Frameworks for Achieving Turn-On/Off of the Catalytic Activity in Different CO₂ Reactions, *Angew. Chem., Int. Ed.*, 2022, **61**, e202200123.

- 6 Y.-R. Wang, H.-M. Ding, S.-N. Sun, J.-W. Shi, Y.-L. Yang, Q. Li, Y. Chen, S.-L. Li and Y.-Q. Lan, Light, Heat and Electricity Integrated Energy Conversion System: Photothermal-Assisted Co-Electrolysis of CO₂ and Methanol, *Angew. Chem., Int. Ed.*, 2022, **61**, e202212162.
- 7 P. Wu, Y. Li, J. Zheng, N. Hosono, K. Otake, J. Wang, Y. Liu, L. Xia, M. Jiang, S. Sakaki and S. Kitagawa, Carbon dioxide capture and efficient fixation in a dynamic porous coordination polymer, *Nat. Commun.*, 2019, **10**, 4362.
- 8 Q. H. Yang, C. C. Yang, C. H. Lin and H.-L. Jiang, Metal-organic-framework-derived hollow N-doped porous carbon with ultrahigh concentrations of single Zn atoms for efficient carbon dioxide conversion, *Angew. Chem., Int. Ed.*, 2019, **58**, 3511–3515.
- 9 M. H. Kim, T. Song, U. R. Seo, J. E. Park, K. Cho, S. M. Lee, H. J. Kim, Y. J. Ko, Y. K. Chung and S. U. Son, Hollow and microporous catalysts bearing Cr(III)-F porphyrins for room temperature CO₂ fixation to cyclic carbonates, *J. Mater. Chem. A*, 2017, **5**, 23612–23619.
- 10 J. Dong, P. Cui, P. F. Shi, P. Cheng and B. Zhao, Ultrastrong alkali-resisting lanthanide-zeolites assembled by [Ln₆₀] nanocages, *J. Am. Chem. Soc.*, 2015, **137**, 15988–15991.
- 11 Y. M. Zhao, Y. L. Peng, C. Shan, Z. Lu, L. Wojtas, Z. J. Zhang, B. Zhang, Y. Q. Feng and S. Q. Ma, Metal-organic-framework-based porous organic polymers as a heterogeneous catalytic nanoplatform for efficient carbon dioxide conversion, *Nano Res.*, 2022, **15**, 1145–1152.
- 12 G. Yuan, Y. Lei, X. Y. Meng, B. D. Ge, Y. Ye, X. W. Song and Z. Q. Liang, Metal-assisted synthesis of salen-based porous organic polymer for highly efficient fixation of CO₂ into cyclic carbonates, *Inorg. Chem. Front.*, 2022, **9**, 1208–1216.
- 13 Z. Dai, Y. Long, J. Liu, Y. Bao, L. Zheng, J. Ma, J. Liu, F. Zhang, Y. Xiong and J.-Q. Lu, Functional Porous Ionic Polymers as Efficient Heterogeneous Catalysts for the Chemical Fixation of CO₂ under Mild Conditions, *Polymers*, 2022, **14**, 2658.
- 14 J.-G. Jia and L.-M. Zheng, Metal-organic nanotubes: Designs, structures and functions, *Coord. Chem. Rev.*, 2020, **403**, 213083.
- 15 P. Thanasekaran, T.-T. Luo, C.-H. Lee and K.-L. Lu, A journey in search of single-walled metal-organic nanotubes, *J. Mater. Chem.*, 2011, **21**, 13140–13149.
- 16 F. Dai, H. He and D. Sun, Polymorphism in High-Crystalline-Stability Metal-Organic Nanotubes, *Inorg. Chem.*, 2009, **48**, 4613–4615.
- 17 K. Otsubo, Y. Wakabayashi, J. Ohara, S. Yamamoto, H. Matsuzaki, H. Okamoto, K. Nitta, T. Uruga and H. Kitagawa, Bottom-up realization of a porous metal-organic nanotubular assembly, *Nat. Mater.*, 2011, **10**, 291–295.
- 18 L. L. Zou, C. C. Hou, Z. Liu, H. Pang and Q. Xu, Superlong single-crystal metal-organic framework nanotubes, *J. Am. Chem. Soc.*, 2018, **140**, 15393–15401.
- 19 T.-T. Luo, H.-C. Wu, Y.-C. Jao, S.-M. Huang, T.-W. Tseng, Y.-S. Wen, G.-H. Lee, S.-M. Peng and K.-L. Lu, Self-Assembled Arrays of Single-Walled Metal-Organic Nanotubes, *Angew. Chem., Int. Ed.*, 2009, **48**, 9461–9464.
- 20 C. R. Murdock and D. M. Jenkins, Isostructural Synthesis of Porous Metal-Organic Nanotubes, *J. Am. Chem. Soc.*, 2014, **136**, 10983–10988.
- 21 Y.-L. Wu, J. Qian, G.-P. Yang, F. Yang, Y.-T. Liang, W.-Y. Zhang and Y.-Y. Wang, High CO₂ Uptake Capacity and Selectivity in a Fascinating Nanotube-Based Metal-Organic Framework, *Inorg. Chem.*, 2017, **56**, 908–913.
- 22 S. Ma, J. M. Simmons, D. Yuan, J.-R. Li, W. Weng, D.-J. Liu and H.-C. Zhou, A nanotubular metal-organic framework with permanent porosity: structure analysis and gas sorption studies, *Chem. Commun.*, 2009, 4049–4051.
- 23 Y.-W. Zhao and X.-M. Zhang, The construction of helicate metal-organic nanotubes and enantioselective recognition, *J. Mater. Chem. C*, 2020, **8**, 4453–4460.
- 24 Q. Zhang, A. Geng, H. Zhang, F. Hu, Z.-H. Lu, D. Sun, X. Wei and C. Ma, An Independent 1D Single-Walled Metal-Organic Nanotube Transformed from a 2D Layer Exhibits Highly Selective and Reversible Sensing of Nitroaromatic Compounds, *Chem. – Eur. J.*, 2014, **20**, 4885–4890.
- 25 L. Wang, X. Chen, Z. Yi, R. Xu, J. Dong, S. Wang, Y. Zhao and Y. Liu, Facile Synthesis of Conductive Metal-Organic Frameworks Nanotubes for Ultrahigh-Performance Flexible NO Sensors, *Small Methods*, 2022, **6**, 2200581.
- 26 D. K. Unruh, K. Gojdas, A. Libo and T. Z. Forbes, Development of Metal-Organic Nanotubes Exhibiting Low-Temperature, Reversible Exchange of Confined “Ice Channels”, *J. Am. Chem. Soc.*, 2013, **135**, 7398–7401.
- 27 T.-W. Tseng, T.-T. Luo, C.-C. Su, H.-H. Hsu, C.-I. Yang and K.-L. Lu, An unusual cobalt(II)-based single-walled metal-organic nanotube, *CrystEngComm*, 2014, **16**, 2626–2633.
- 28 Y. Sun, D.-F. Lu, K. Wu, T. Zhou, F. Wang and J. Zhang, Construction of Metal-Organic Frameworks with Various Zinc-Tetrazolate Nanotubes, *Cryst. Growth Des.*, 2021, **21**, 28–32.
- 29 Y. Wei, D. Sun, D. Yuan, Y. Liu, Y. Zhao, X. Li, S. Wang, J. Dou, X. Wang, A. Hao and D. Sun, Pb(II) metal-organic nanotubes based on cyclodextrins: biphasic synthesis, structures and properties, *Chem. Sci.*, 2012, **3**, 2282–2287.
- 30 Y. Zhou, S. Yao, Y. Ma, G. Li, Q. Huo and Y. Liu, An anionic single-walled metal-organic nanotube with an armchair (3,3) topology as an extremely smart adsorbent for the effective and selective adsorption of cationic carcinogenic dyes, *Chem. Commun.*, 2018, **54**, 3006–3009.
- 31 F. Dai, H. He and D. Sun, A Metal-Organic Nanotube Exhibiting Reversible Adsorption of (H₂O)₁₂ Cluster, *J. Am. Chem. Soc.*, 2008, **130**, 14064–14065.
- 32 J. Tian, L. Liu, K. Zhou, Z. Hong, Q. Chen, F. Jiang, D. Yuan, Q. Sun and M. Hong, Metal-organic tube or layered assembly: reversible sheet-to-tube transformation and adaptive recognition, *Chem. Sci.*, 2020, **11**, 9818–9826.
- 33 L.-L. Chen, Y.-Y. Wu, W.-W. Wu, M.-M. Wang, H.-J. Lun, D.-B. Dang, Y. Bai and Y.-M. Li, Ultrastable

- Polyoxometalate-Encapsulated Supramolecular Metal–Organic Nanotubes for Single-Crystal Proton Conduction, *Inorg. Chem.*, 2022, **61**, 8629–8633.
- 34 G.-Q. Kong, S. Ou, C. Zou and C.-D. Wu, Assembly and Post-Modification of a Metal–Organic Nanotube for Highly Efficient Catalysis, *J. Am. Chem. Soc.*, 2012, **134**, 19851–19857.
- 35 Z. Zhou, C. He, J. Xiu, L. Yang and C. Duan, Metal–Organic Polymers Containing Discrete Single-Walled Nanotube as a Heterogeneous Catalyst for the Cycloaddition of Carbon Dioxide to Epoxides, *J. Am. Chem. Soc.*, 2015, **137**, 15066–15069.
- 36 Z. Gao, L. Liang, X. Zhang, P. Xu and J. Sun, Facile One-Pot Synthesis of Zn/Mg-MOF-74 with Unsaturated Coordination Metal Centers for Efficient CO₂ Adsorption and Conversion to Cyclic Carbonates, *ACS Appl. Mater. Interfaces*, 2021, **13**, 61334–61345.
- 37 V. A. Blatov, *The topological analysis has been done by using the ToposPro program with version 5.4.3.0*, IUCr CompComm, Newsletter 2006, 7, 4.
- 38 K. Takaishi, T. Okuyama, S. Kadosaki, M. Uchiyama and T. Ema, Hemisquaramide tweezers as organocatalysts: Synthesis of cyclic carbonates from epoxides and CO₂, *Org. Lett.*, 2019, **21**, 1397–1401.
- 39 M. Liu, P. Zhao, R. Ping, F. Liu, F. Liu, J. Gao and J. Sun, Squaramide-derived framework modified periodic mesoporous organosilica: A robust bifunctional platform for CO₂ adsorption and cooperative conversion, *Chem. Eng. J.*, 2020, **399**, 125682.
- 40 Y. Hu, X. Hao, Z. Cui, J. Zhou, S. Chu, Y. Wang and Z. Zou, Enhanced photocarrier separation in conjugated polymer engineered CdS for direct Z-scheme photocatalytic hydrogen evolution, *Appl. Catal., B*, 2020, **260**, 118131.
- 41 W.-Y. Gao, Y. Chen, Y. Niu, K. Williams, L. Cash, P. J. Perez, L. Wojtas, J. Cai, Y.-S. Chen and S. Ma, Crystal Engineering of an nbo Topology Metal–Organic Framework for Chemical Fixation of CO₂ under Ambient Conditions, *Angew. Chem., Int. Ed.*, 2014, **53**, 2615–2619.
- 42 J. Liang, R.-P. Chen, X.-Y. Wang, T.-T. Liu, X.-S. Wang, Y.-B. Huang and R. Cao, Postsynthetic ionization of an imidazole-containing metal–organic framework for the cycloaddition of carbon dioxide and epoxides, *Chem. Sci.*, 2017, **8**, 1570–1575.
- 43 Z. Helwani, A. D. Wiheeb, J. Kim and M. R. Othman, *In situ* Mineralization of Carbon Dioxide in a Coal-Fired Power Plant, *Energy Sources, Part A*, 2016, **38**, 606–611.
- 44 X. Guo, Z. Zhou, C. Chen, J. Bai, C. He and C. Duan, New rht-Type Metal–Organic Frameworks Decorated with Acylamide Groups for Efficient Carbon Dioxide Capture and Chemical Fixation from Raw Power Plant Flue Gas, *ACS Appl. Mater. Interfaces*, 2016, **8**, 31746–3va1756.
- 45 X. C. Xu, C. S. Song, R. Wincek, J. M. Andresen, B. G. Miller and A. W. Scaroni, Separation of CO₂ from Power Plant Flue Gas Using a Novel CO₂ “Molecular Basket” Adsorbent, *Fuel Chem. Div. Prepr.*, 2003, **48**, 162–163.